

1 A butterfly chromonome reveals selection dynamics during extensive and  
2 cryptic chromosomal reshuffling

3

4

5 Authors

6

7 Jason Hill<sup>1,†</sup>, Ramprasad Neethiraj<sup>1</sup>, Pasi Rastas<sup>2</sup>, Nathan Clark<sup>3</sup>, Nathan Morehouse<sup>4</sup>, Maria de la

8 Paz Celorio-Mancera<sup>1</sup>, Jofre Carnicer Cols<sup>5,6</sup>, Heinrich Dircksen<sup>10</sup>, Camille Meslin<sup>3</sup>, Kristin

9 Sikkink<sup>7</sup>, Maria Vives<sup>5,6</sup>, Heiko Vogel<sup>9</sup>, Christer Wiklund<sup>1</sup>, Carol L. Boggs<sup>8</sup>, Sören Nylin<sup>1</sup>,

10 Christopher Wheat<sup>1,†</sup>

11 Affiliations:

12 1 Population Genetics, Department of Zoology, Stockholm University, Stockholm, Sweden

13 2 Institute of Biotechnology, (DNA Sequencing and Genomics), University of Helsinki, Helsinki,

14 Finland

15 3 Department of Computational and Systems Biology, University of Pittsburgh, Pittsburgh, USA

16 4 Department of Biological Sciences, University of Cincinnati, Cincinnati, USA

17 5 Department of Evolutionary Biology, Ecology and Environmental Sciences, University of

18 Barcelona, 08028 Barcelona, Spain

19 6 CREAM, Global Ecology Unit, Autonomous University of Barcelona, 08193 Cerdanyola del

20 Vallès, Spain

21 7 Department of Ecology, Evolution and Behavior, University of Minnesota, St Paul, MN, USA

22 8 Department of Biological Sciences University of South Carolina, Columbia, SC, USA

23 9 Department of Entomology, Max Planck Institute for Chemical Ecology, D-07745 Jena, Germany

24 10 Functional Morphology, Department of Zoology, Stockholm University, Stockholm, Sweden

25

26 <sup>‡</sup> Authors for correspondence:

27 Jason Hill <jason.hill@zoologi.su.se>

28 Christopher Wheat <chris.wheat@zoologi.su.se>

29

## 30 **Abstract**

31 Taxonomic orders vary in their degree of chromosomal conservation with some having high  
32 rates of chromosome number turnover despite maintaining some core sets of ordered genes (e.g.  
33 Mammalia) and others exhibiting rapid rates of gene-order reshuffling without changing  
34 chromosomal count (e.g. Diptera). However few clades exhibit as much conservation as the  
35 Lepidoptera for which both chromosomal count and gene colinearity (synteny) are very high over  
36 the past 140 MY. In contrast, here we report extensive chromosomal rearrangements in the genome  
37 of the green-veined white butterfly (*Pieris napi*, Pieridae, Linnaeus, 1758). This unprecedented  
38 reshuffling is cryptic: microsynteny and chromosome number do not indicate the extensive  
39 rearrangement revealed by a chromosome level assembly and high-resolution linkage map.  
40 Furthermore, the rearrangement blocks themselves appear to be non-random, as they are  
41 significantly enriched for clustered groups of functionally annotated genes revealing that the  
42 evolutionary dynamics acting on Lepidopteran genome structure are more complex than previously  
43 envisioned.

## 44 **Introduction**

45 The role of chromosomal rearrangements in adaptation and speciation has long been  
46 appreciated and recent work has elevated the profile of supergenes in controlling complex adaptive  
47 phenotypes<sup>1-4</sup>. Chromosome number variation has also been cataloged for many species but  
48 analyses of the adaptive implications have mostly been confined to the consequences of polyploidy  
49 and whole genome duplication<sup>5,6</sup>. The identification of pervasive fission and fusion events  
50 throughout the genome is relatively unexplored since discovery of this pattern requires chromosome

51 level assemblies. This leaves open the possibility of cryptic chromosomal dynamics taking place in  
52 many species for which this level of genome assembly has not been achieved. As chromosomal  
53 levels assemblies become more common, uncovering a relationship between such dynamics and  
54 adaptation or speciation can be assessed.

55 Here we focus upon the Lepidoptera, the second most diverse animal group with over 160,000  
56 extant species in more than 160 families. Butterflies and moths exist in nearly all habitats and have  
57 equally varied life histories yet show striking similarity in genome architecture, with the vast  
58 majority having a haploid chromosome number of  $n=31^{7-9}$ . While haploid chromosome number can  
59 vary from  $n = 5$  to  $n = 223^{10-12}$ , gene order and content is remarkably similar within chromosomes  
60 (i.e. displays macrosynteny), regardless of haploid chromosome number. The degree of such  
61 synteny between species separated by up to 140 My is astounding as illustrated by recent  
62 chromosomal level genomic assemblies<sup>7,13</sup>, as well as previous studies of the sequence and structure  
63 of lepidopteran genomes<sup>14-17</sup>. This ability of Lepidoptera to accommodate such chromosomal  
64 rearrangements, yet maintain high levels of macro and microsynteny (i.e. collinearity at the scale of  
65 10s to 100's of genes) is surprising. While a growing body of evidence indicates that gene order in  
66 eukaryotes is non-random along chromosomes, with upwards of 12% of genes organized into  
67 functional neighborhoods of shared function and expression patterns<sup>18,19</sup>, to what extent this may  
68 play a role in the chromosomal evolution is an open question.

69 Variation in patterns of synteny across clades must arise due to an evolutionary interaction between  
70 selection and constraint<sup>20</sup>, likely at the level of telomere and centromere performance. *Drosophila*,  
71 and likely all Diptera, differ from other eukaryotes studied to date in lacking the telomerase  
72 enzyme, and instead protect their chromosomal ends using retrotransposons<sup>21</sup>. This absence of  
73 telomerase is posited to make evolving novel telomeric ends more challenging, limiting the  
74 appearance of novel chromosomes and thereby resulting in high macrosynteny via constraint<sup>22</sup>.

75 In contrast, Lepidoptera like most Metazoans use telomerase to protect their chromosomal ends  
76 which allows for previously internal chromosomal DNA to become subtelomeric in novel

77 chromosomes<sup>7,13</sup>. Additionally all Lepidoptera have holocentric chromosomes in which the  
78 decentralized kinetochore allows for more rearrangements by fission, fusion, and translocation of  
79 chromosome fragments than is the case for monocentric chromosomes<sup>23</sup>. Thus, Lepidoptera should  
80 be able to avoid the deleterious consequences of large-scale chromosomal changes.

81 Here we present the chromosome level genome assembly of the green-veined white butterfly *P.*  
82 *napi*. Our analysis reveals large-scale fission and fusion events similar to known dynamics in other  
83 lepidopteran species but at an accelerated rate and without a change in haploid chromosome count.  
84 The resulting genome-wide breakdown of the chromosome level synteny is unique among  
85 Lepidoptera. While we are unable to identify any repeat elements associated with this cryptic  
86 reshuffling, we find the chromosomal ends reused and the collinearity of functionally related genes.  
87 These findings support a reinterpretation of the chromosomal fission dynamics in the Lepidoptera.

88

## 89 Results

90 The *P. napi* genome was generated using DNA from inbred siblings from Sweden, a genome  
91 assembly using variable fragment size libraries (180 bp to 100 kb; N50-length of 4.2 Mb and a total  
92 length of 350 Mb), and a high density linkage map across 275 full-sib larva, which placed 122  
93 scaffolds into 25 linkage groups, consistent with previous karyotyping of *P. napi*<sup>24,25</sup>. After  
94 assessment and correction of the assembly, the total chromosome level assembly was 299 Mb  
95 comprising 85% of the total assembly size and 114% of the k-mer estimated haploid genome size,  
96 with 2943 scaffolds left unplaced (**Supplementary Note 3**). Subsequent annotation predicted  
97 13,622 gene models, 9,346 with functional predictions (**Supplementary Note 4**).

98 Single copy orthologs (SCOs) in common between *P. napi* and the first sequenced  
99 Lepidopteran genome, the silk moth *Bombyx mori* (Bombycidae), were identified. These revealed  
100 an unexpected deviation in gene order and chromosomal structure in *P. napi* relative to *B. mori* as  
101 well as another lepidopteran genome with a linkage map and known chromosomal structure, that of

102 *Heliconius melpomene* (Nymphalidae) (Fig 1a). Large-scale rearrangements that appeared to be the  
103 fission and subsequent fusion of fragments on the scale of megabases were present on every *P. napi*  
104 chromosome relative to *B. mori*, *H. melpomene*, and *Melitaea cinxia* (Nymphalidae) (fig 1b). We  
105 characterized the size and number of large scale rearrangements between *P. napi* and *B. mori* using  
106 shared SCOs to identify 99 clearly defined blocks of co-linear gene order (hereafter referred to as  
107 “syntenic blocks”), with each syntenic block having an average of 69 SCOs. Each *P. napi*  
108 chromosome contained an average of 3.96 (SD = 1.67) syntenic blocks, which derived on average  
109 from 3.5 different *B. mori* chromosomes. In *P. napi*, the average syntenic block length was 2.82 Mb  
110 (SD = 1.97 Mb) and contained 264 genes (SD = 219).

111 The indication that *P. napi* diverged radically from the thus far observed chromosomal  
112 structure of lepidopterans raised questions about how frequently a *P. napi* like chromosomal  
113 structure is observed vs. the structure reported in the highly syntenic *B. mori*, *H. melpomene*, and  
114 *M. cinxia* genomes. We accessed 22 publicly available lepidopteran genome assemblies and their  
115 gene annotations representing species that diverged up to 140 MYA in order to identify the genes  
116 corresponding to the SCO’s used in the previous analyses. We used blastx (Diamond v0.9.10)<sup>26</sup> to  
117 place those genes on their native species scaffolds. With informations about each SCO’s location on  
118 the *P. napi* and *B. mori* chromosomes we recorded how often a scaffold contained a cluster of genes  
119 whose orthologs resided on two *P. napi* chromosomes or two *B. mori* chromosomes. If two *P. napi*  
120 chromosomes were represented by only a single *B. mori* chromosome, then the scaffold was marked  
121 as containing an mori-like join. Conversely if two *B. mori* chromosomes were represented but only  
122 a single *P. napi* chromosome, then the scaffold was marked as containing a napi-like join. In total  
123 we found that 20 species have more mori-like joins, and two species of *Pieris* represented by 3  
124 assemblies have more napi-like joins (Fig 2a). While this type of assessment is preliminary the  
125 indication is that the genome structure described here is novel to the genus *Pieris*.

126 We validated this novel chromosomal reorganization using four complementary but  
127 independent approaches to assess our scaffold joins. First, we generated a second linkage map for *P.*

128 *napi*, which confirmed the 25 linkage groups and the ordering of scaffold joins along chromosomes  
129 (Fig. 3; Supplementary Fig. 2). Second, the depth of the mate-pair (MP) reads spanning joins  
130 indicated by the first linkage map provides an independent assessment of the join validity. We  
131 therefore quantified MP reads spanning each base pair position along a chromosome (Fig. 3;  
132 Supplementary Fig. 2, Note 7), finding strong support for the scaffold joins. Third, we aligned the  
133 scaffolds of a recently constructed genome of *P. rapae*<sup>27</sup> to *P. napi*, looking for *P. rapae* scaffolds  
134 that spanned the chromosomal level scaffold joins within *P. napi*, finding support for 71 of the 97  
135 joins (Supplementary Fig. 5). Fourth, we considered *B. mori* syntenic blocks that spanned a scaffold  
136 join within a *P. napi* chromosome as support for that *P. napi* chromosome assembly, and found that  
137 62 of the 97 scaffold joins were supported by *B. mori* (Supplementary Fig. 2, Note 8,9).

138         To assess the novel chromosomal organization, we investigated the ordering and content of  
139 these syntenic blocks in *P. napi*. First, we tested whether telomeric ends of chromosomes were at all  
140 conserved between species despite the extensive chromosomal reshuffling (Fig. 4a). We found  
141 significantly more syntenic blocks sharing telomere facing orientations between species than  
142 expected ( $P < 0.01$ , two tailed t-test; Fig. 4b). We also identified a significant enrichment for SCOs  
143 in *B. mori* and *P. napi* located at roughly similar distance from the end of their respective  
144 chromosomes (Fig. 4c). Both of these findings are consistent with the ongoing use of telomeric  
145 ends, indicating that strong selection dynamics have favored their retention over evolutionary time.  
146 Second, we tested for gene set functional enrichment within the observed syntenic blocks by  
147 investigating the full set of annotated *P. napi* genes. We found that 57 of the 99 block regions in the  
148 *P. napi* genome contained at least three genes with a shared gene ontology (GO) term that was  
149 significantly less frequent in the rest of the genome ( $P < 0.01$ , fisher) (Supplementary fig. 3). We  
150 then tested whether the observed enrichment in the syntenic blocks of *P. napi* was greater than  
151 expected by randomly assigning the genome into similarly sized blocks. The mean number of GO  
152 enriched fragments in each of the simulated 10,000 genomes was 38.8 (variance of 46.6 and  
153 maximum of 52), which was significantly lower than the observed ( $P < 0.0001$ ).

154 To assess the possible cause of the reshuffling, we surveyed the distribution of different  
155 repeat element classes across the genome, looking for enrichment of specific categories near the  
156 borders of syntenic blocks. While Class 1 transposons were found to be at higher density at near the  
157 ends of chromosomes relative to the distribution internally (Supplementary fig. 4), no repeat  
158 elements were enriched relative to the position of syntenic block regions. We therefore investigated  
159 whether any repeat element classes had expanded within *Pieris* compared to other sequenced  
160 genomes by assessing the distribution of repeat element classes and genome size among sequenced  
161 Lepidoptera genomes. In accordance with other taxa<sup>28</sup> we find an expected strong relationship  
162 between genome size and repetitive element content in *Pieris* species. Thus, while repetitive  
163 elements such as transposable elements are likely to have been involved in the reshuffling, our  
164 inability to find clear elements involved suggests these events may be old and their signal decayed.

## 165 **Methods**

166 **Sample collection and DNA extraction.** Pupal DNA was isolated from a 4th generation inbred  
167 cohort that originated from a wild caught female collected in Skåne, Sweden, using a standard salt  
168 extraction<sup>29</sup>.

169 **Illumina genome sequencing.** Illumina sequencing was used for all data generation used in  
170 genome construction. A 180 paired end (PE) and the two mate pair (MP) libraries were constructed  
171 at Science for Life Laboratory, the National Genomics Infrastructure, Sweden (SciLifeLab), using 1  
172 PCR-free PE DNA library (180bp) and 2 Nextera MP libraries (3kb and 7kb) all from a single  
173 individual. All sequencing was done on Illumina HiSeq 2500 High Output mode, PE 2x100bp by  
174 SciLifeLab. An additional two 40kb MP fosmid jumping libraries were constructed from a sibling  
175 used in the previous library construction. Genomic DNA, isolated as above, was shipped to Lucigen  
176 Co. (Middleton, WI, USA) for the fosmid jumping library construction and sequencing was  
177 performed on an Illumina MiSeq using 2x250bp reads<sup>30</sup>. Finally, a variable insert size library of  
178 100 bp – 100,000 bp in length were generated using the Chicago and HiRise method<sup>31</sup>. Genomic  
179 DNA was again isolated from a sibling of those used in previous library construction. The genomic

180 DNA was isolated as above and shipped to Dovetail Co. (Santa Cruz, CA, USA) for library  
181 construction, sequencing and scaffolding. These library fragments were sequenced by Centillion  
182 Biosciences Inc. (Palo Alto, CA, USA) using Illumina HiSeq 2500 High Output mode, PE 2x100bp.

183 **Data Preparation and Genome assembly.** Nearly 500 M read pairs of data were generated,  
184 providing ~ 285 X genomic coverage (Supplemental Table 1). The 3kb and 7kb MP pair libraries  
185 were filtered for high confidence true mate pairs using Nextclip v0.8<sup>32</sup>. All read sets were then  
186 quality filtered, the ends trimmed of adapters and low quality bases, and screened of common  
187 contaminants using bbduk v37.51 (bbtools, Brian Bushnell). Insert size distributions were plotted to  
188 assess library quality, which was high (Supplementary Fig. 1). The 180bp, 3kb, and 7kb, read data  
189 sets were used with AllpathsLG r50960<sup>33</sup> for initial contig generation and scaffolding  
190 (Supplementary Note 1). AllpathsLG was run with haploidify = true to compensate for the high  
191 degree of heterozygosity. The initial contig assembly's conserved single copy ortholog content was  
192 assessed at 78% for *P. napi* by CEGMA v2.5<sup>34</sup>. A further round of superscaffolding using the 40kb  
193 libraries alongside the 3kb and 7kb libraries was done using SSPACE v2<sup>35</sup>. Finally, both assemblies  
194 were Ultascaffolded using the Chicago read libraries and the HiRise software pipeline. These steps  
195 produced a final assembly of 3005 scaffolds with an N50-length of 4.2 Mb and a total length of 350  
196 Mb (Supplementary Note 1).

197 **Linkage Map.** RAD-seq data of 5463 SNP markers from 275 full-sib individuals, without parents,  
198 was used as input into Lep-MAP2<sup>36</sup>. The RAD-seq data was generated from next-RAD technology  
199 by SNPsaurus (Oregon, USA)(Supplemental note 10). To obtain genotype data, the RAD-seq data  
200 was mapped to the reference genome using BWA mem<sup>37</sup> and SAMtools<sup>38</sup> was used to produce  
201 sorted bam files of the read mappings. Based on read coverage (samtools depth), Z chromosomal  
202 regions were identified from the genome and the sex of offspring was determined. Custom scripts<sup>39</sup>  
203 were used to produce genotype likelihoods (called posteriors in Lep-MAP) from the output of  
204 SAMtools mpileup.



205 The parental genotypes were inferred with Lep-MAP2 ParentCall module using parameters  
206 "ZLimit=2 and ignoreParentOrder=1", first calling Z markers and second calling the parental  
207 genotypes by ignoring which way the parents are informative (the parents were not genotyped so  
208 we could not separate maternal and paternal markers at this stage). Scripts provided with Lep-  
209 MAP2 were used to produce linkage file from the output of ParentCall and all single parent  
210 informative markers were converted to paternally informative markers by swapping parents, when  
211 necessary. Filtering by segregation distortion was performed using Filtering module.

212 Following this, the SeparateChromosomes module was run on the linkage file and 25 chromosomes  
213 were identified using LOD score limit 39. Then JoinSingles module was run twice to add more  
214 markers on the chromosomes with LOD score limit of 20. Then SeparateChromosomes was run  
215 again but only on markers informative on single parent with LOD limit 10 to separate paternally  
216 and maternally informative markers. 51 linkage groups were found and all were ordered using  
217 OrderMarkers module. Based on likelihood improvement of marker ordering, paternal and maternal  
218 linkage groups were determined. This was possible as there is no recombination in females  
219 (achiasmatic meiosis), and thus the order of the markers does not improve likelihood on the female  
220 map. The markers on the corresponding maternal linkage groups were converted to maternally  
221 informative and OrderMarkers was run on the resulting data twice for each of 25 chromosomes  
222 (without allowing recombination in female). The final marker order was obtained as the order with  
223 the higher likelihood from the two runs.

224 **Chromosomal assembly.** The 5463 markers that composed the linkage map were mapped to the *P.*  
225 *napi* ultrascaffolds using bbmap<sup>40</sup> with sensitivity = slow. Reads that mapped uniquely were used to  
226 identify misassemblies in the Ultrascaffolds and arrange those fragments into chromosomal order.  
227 54 misassemblies were identified and overall 115 fragments were joined together into 25  
228 chromosomes using a series of custom R scripts (supplemental information) and the R package  
229 Biostrings<sup>41</sup>. Scaffold joins and misassembly corrections were validated by comparing the number  
230 of correctly mapped mate pairs spanning a join between two scaffolds. Mate pair reads from the

231 3kb, 7kb, and 40kb libraries were mapped to their respective assemblies with bbmap (po=t,  
232 ambig=toss, kbp=t). SAM output was filtered for quality and a custom script was used to tabulate  
233 read spanning counts for each base pair in the assembly.

234 **Synteny Comparisons Between *P. napi*, *B. mori*, and *H. melpomene*.** A list of 3100 single copy  
235 orthologs (SCO) occurring in the Lepidoptera lineage curated by OrthoDB v9.1<sup>42</sup> was used to  
236 extract gene names and protein sequences of SCOs in *Bombyx mori* from  
237 KaikoBase<sup>43</sup> (Supplemental Note 5) using a custom script. Reciprocal best hits (RBH) between gene  
238 sets of *P. napi*, *P. rapae*, *H. melpomene*, *M. cinxia*, and *B. mori* SCOs were identified using  
239 BLASTP<sup>44</sup> and custom scripts. Gene sets of *H. melpomene* v2.5 and *M. cinxia* v1 were downloaded  
240 from LepBase v4<sup>45</sup>. Coordinates were converted to chromosomal locations and visualized using  
241 Circos<sup>46</sup> and custom R scripts.

242 **Synteny Comparison Within Lepidoptera.** Genome assemblies and annotated protein sets were  
243 downloaded for 24 species of Lepidoptera from LepBase v4<sup>47</sup> and other sources (Supplemental  
244 Table 4). Each target species protein set was aligned to its species genome as well as to the *Pieris*  
245 *napi* protein set using Diamond v0.9.10<sup>26</sup> with default options. The protein-genome comparison was  
246 used to assign each target species gene to one of its assembled scaffolds, while the protein-protein  
247 comparison was used to identify RBHs between the protein of each species and its ortholog in *P.*  
248 *napi*, and *B. mori*. Using this information we used a custom R script to examine each assembly  
249 scaffold for evidence of synteny to either *P. napi* or *B. mori*. First, each scaffold of the target species  
250 genome was assigned genes based on the protein-genome blast results, using its own protein set and  
251 genome. A gene was assigned to a scaffold if at least 3 HSPs of less than 200bp from a gene aligned  
252 with  $\geq 95\%$  identity. Second, if any of these scaffolds then contained genes whose orthologs  
253 resided on a single *B. mori* chromosome but two *P. napi* chromosomes, and those same two *P. napi*  
254 chromosome segments were also joined in the *B. mori* assembly, that was counted as a ‘mori-like  
255 join’. Conversely if a target species scaffold contained genes whose orthologs resided on a single *P.*

256 *napi* chromosome but two *B. mori* chromosomes, and those same two *B. mori* chromosome  
257 segments were also joined in the *P. napi* assembly, that was counted as a ‘napi-like join’.

## 258 **Pieridae chromosomal evolution.**

259 Chromosomal fusions and fissions were reconstructed across the family Pieridae by placing  
260 previously published karyotype studies of haploid chromosomal counts into their evolutionary  
261 context. There are approximately 1000 species in the 85 recognized genera of Pieridae and we  
262 recently reconstructed a robust fossil-calibrated chronogram for this family at the genus level<sup>48,49</sup>.  
263 We then placed the published chromosomal counts for 201 species<sup>9,50</sup> on this time calibrated  
264 phylogeny with ancestral chromosomal reconstructions for chromosome count, treated as a  
265 continuous character, using the contMap function of the phytools R package<sup>51</sup>.

266 **Second Linkage Map for *P. napi*.** A second linkage map was constructed from a different family  
267 of *P. napi* in which a female from Abisko, Sweden was crossed with a male from Catalonia, Spain.  
268 Genomic DNA libraries were constructed for the mother, father, and four offspring (2 males, 2  
269 females). RNA libraries were constructed for an additional 6 female and 6 male offspring. All  
270 sequencing was performed on a Illumina HiSeq 2500 platform using High Output mode, with PE  
271 2x100bp reads at SciLifeLab (Stockholm, Sweden). Both DNA and RNA reads were mapped to the  
272 genome assembly with bbmap. Samtools was used to sort read mappings and merge them into an  
273 mpileup file (Supplemental Note 6). Variants were called with BCFtools<sup>52</sup> and filtered with  
274 VCFtools<sup>53</sup>. Linkage between SNPs was assessed with PLINK<sup>54</sup>. A custom script was used to assess  
275 marker density and determine sex-specific heterozygosity.

276 **Annotation of *P. napi* genome.** Genome annotation was carried out by the Bioinformatics Short-  
277 term Support and Infrastructure (BILS, Sweden). BILS was provided with the chromosomal  
278 assembly of *P. napi* and 45 RNAseq read sets representing 3 different tissues (head, fat body, and  
279 gut) of 7 male and 8 female larva from lab lines were separate from the one used for the initial  
280 sequencing. Sequence evidence for the annotation was collected in two complementary ways. First,

281 we queried the Uniprot database<sup>55</sup> for protein sequences belonging to the taxonomic group of  
282 Papilionoidea (2,516 proteins). In order to be included, proteins gathered in this way had to be  
283 supported on the level of either proteomics or transcriptomics and could not be fragments. In  
284 addition, we downloaded the Uniprot-Swissprot reference data set (downloaded on 2014-05-15)  
285 (545,388 proteins) for a wider taxonomic coverage with high-confidence proteins. In addition, 493  
286 proteins were used that derived from a *P. rapae* expressed sequence tag library that was Sanger  
287 sequenced.

288 **Permutation test of syntenic block position within chromosomes.** Syntenic blocks (SBs) were  
289 identified as interior vs terminal and the ends of terminal blocks were marked as inward or outward  
290 facing. SBs were reshuffled into 25 random chromosomes of 4 SBs in a random orientation and the  
291 number of times that a terminal block occurred in a random chromosome with the outward end  
292 facing outward was counted. This was repeated 10,000 times to generate a random distribution  
293 expectation. The number of terminal outward-facing SBs in *B. mori* that were also terminal and  
294 outward facing in *P. napi* was compared to this random distribution to derive the significance of  
295 deviation from the expected value. To test the randomness of gene location within chromosomes,  
296 orthologs were numbered by their position along each chromosome in both *B. mori* and *P. napi*.  
297 10,000 random genomes were generated as above. Distance from the end of the new chromosome  
298 and distance from the end of *B. mori* chromosome were calculated for each ortholog and the results  
299 were binned. P-values were determined by comparing the number of orthologs in a bin to the  
300 expected distribution of genes in a bin from the random genomes. All test were done using a custom  
301 R script.

302 **Gene set enrichment analysis of syntenic blocks.** Gene ontology set enrichment was initially  
303 tested within syntenic blocks of the *P. napi* genome using topGO<sup>56</sup> with all 13,622 gene models  
304 generated from the annotation. For each syntenic block within the genome, each GO term of any  
305 level within the hierarchy that had at least 3 genes belonging to it was analyzed for enrichment. If a  
306 GO term was overrepresented in a syntenic block compared to the rest of the genome at a p-value of

307 < 0.01 by a Fisher exact test, that block was counted as enriched. 57 of the 99 syntenic blocks in the  
308 *P. napi* genome were enriched in this way. Because arbitrarily breaking up a genome and testing for  
309 GO enrichment can yield results that are dependent on the distribution of the sizes used, we  
310 compared the results of the previous analysis to the enrichment found using the same size genomic  
311 regions, randomly selected from the *P. napi* genomes. The size distribution of the 99 syntenic  
312 blocks were used to generate fragment sizes into which the genome was randomly assigned. This  
313 resulted in a random genome of 99 fragments which in total contained the entire genome but the  
314 content of a given fragment was random compared to the syntenic block that defined its size. This  
315 random genome was tested for GO enrichment of the fragments in the same way as the syntenic  
316 blocks in the original genome, and the number of enriched blocks counted. This was then repeated  
317 10,000 times to generate a distribution of expected enrichment in genome fragments of the same  
318 size as the *P. napi* syntenic blocks.

319

## 320 **Discussion**

321 While massive chromosomal fission events are well documented in butterflies (e.g.  
322 *Leptidea* in Pieridae (n=28-103); *Agrodiaetus* in Lycaenidae (n=10-134)), their contribution to  
323 Lepidopteran diversity appears to be minimal as all these clades are very young<sup>57-59</sup>. However, our  
324 results challenge this interpretation. Rather, *P. napi* appears to represent a lineage that has  
325 undergone an impressive reconciliation of an earlier series of rampant fission events. Moreover, the  
326 subsequent fusion events exhibit a clear bias toward using ancient telomeric ends, as well as  
327 returning gene clusters to their relative ancestral position within chromosomes even when the other  
328 parts of the newly formed chromosome originated from other sources. Luckily these initial fission  
329 events have been frozen in time as reshuffled syntenic blocks, revealing the potential fitness  
330 advantage of maintaining certain functional categories as syntenic blocks.

331 Thus, despite the potential for holocentric species to have relaxed constraint upon their  
332 chromosomal evolution, we find evidence for selection actively maintaining ancient telomeric ends,  
333 as well as gene order within large chromosomal segments. Together these observations suggest that  
334 the low chromosome divergence in Lepidoptera over > 100 million generations is at least partially  
335 due to purifying selection maintaining an adaptive chromosomal structure.

336

## 337 **Bibliography**

338

- 339 1. Schwander, T., Libbrecht, R. & Keller, L. Supergenes and complex phenotypes. *Curr. Biol.*  
340 **24**, R288–R294 (2014).
- 341 2. Kunte, K. *et al.* Doublesex Is a Mimicry Supergene. *Nature* **507**, 229–232 (2014).
- 342 3. Fishman, L., Stathos, A., Beardsley, P. M., Williams, C. F. & Hill, J. P. Chromosomal  
343 rearrangements and the genetics of reproductive barriers in mimulus (monkey flowers).  
344 *Evolution (N. Y.)*. **67**, 2547–2560 (2013).
- 345 4. Lamichhaney, S. *et al.* Structural genomic changes underlie alternative reproductive  
346 strategies in the ruff (*Philomachus pugnax*). *Nat. Genet.* **48**, 84–88 (2015).
- 347 5. Otto, S. P. & Whitton, J. Polyploid Incidence and Evolution. *Annu. Rev. Genet.* **34**, 401–437  
348 (2000).
- 349 6. Van de Peer, Y., Mizrachi, E. & Marchal, K. The evolutionary significance of polyploidy.  
350 *Nat. Rev. Genet.* **18**, 411–424 (2017).
- 351 7. Ahola, V. *et al.* The Glanville fritillary genome retains an ancient karyotype and reveals  
352 selective chromosomal fusions in Lepidoptera. *Nat Commun* **5**, 1–9 (2014).
- 353 8. Lukhtanov, V. A. Sex chromatin and sex chromosome systems in nonditrysian Lepidoptera  
354 (Insecta). *J. Zool. Syst. Evol. Res.* **38**, 73–79 (2000).
- 355 9. ROBINSON, R. *Lepidoptera Genetics. Lepidoptera Genetics* (1971). doi:10.1016/B978-0-  
356 08-006659-2.50017-1
- 357 10. Brown, K. S., Von Schoultz, B. & Suomalainen, E. Chromosome evolution in Neotropical  
358 Danainae and Ithomiinae (Lepidoptera). *Hereditas* **141**, 216–236 (2004).
- 359 11. Kandul, N. P., Lukhtanov, V. A. & Pierce, N. E. Karyotypic diversity and speciation in  
360 *Agrodiaetus* butterflies. *Evolution (N. Y.)*. **61**, 546–559 (2007).
- 361 12. Saura, A., Schoultz, B. Von, Saura, A. O. & Brown, K. S. Chromosome evolution in  
362 Neotropical butterflies. *Hereditas* **150**, 26–37 (2013).

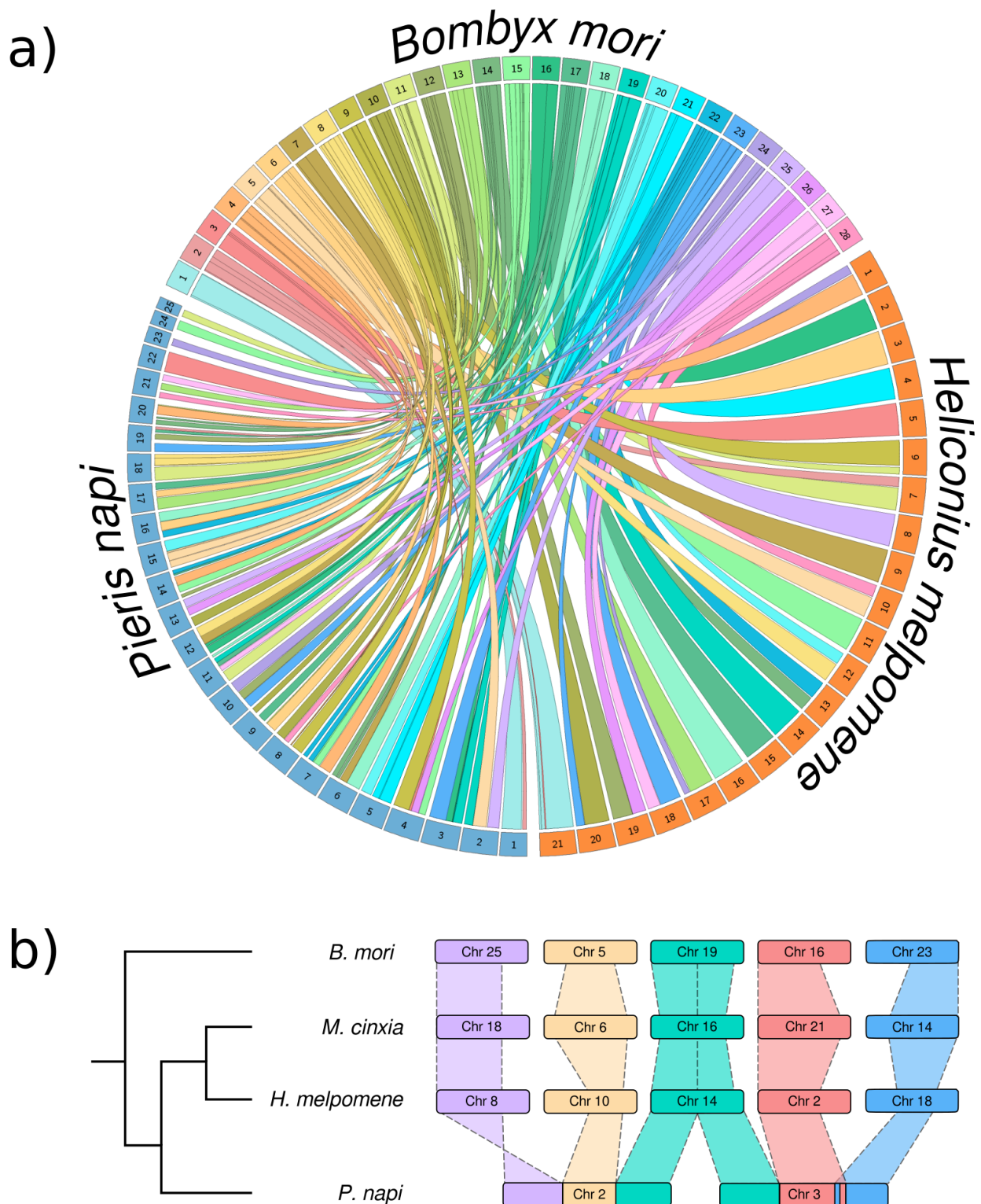
- 363 13. Davey, J. W. *et al.* Major Improvements to the *Heliconius melpomene* Genome Assembly  
364 Used to Confirm 10 Chromosome Fusion Events in 6 Million Years of Butterfly Evolution.  
365 *Genes|Genomes|Genetics* **6**, 695–708 (2016).
- 366 14. Yasukochi, Y. A Second-Generation Integrated Map of the Silkworm Reveals Synteny and  
367 Conserved Gene Order Between Lepidopteran Insects. *Genetics* **173**, 1319–1328 (2006).
- 368 15. Yasukochi, Y. *et al.* A FISH-based chromosome map for the European corn borer yields  
369 insights into ancient chromosomal fusions in the silkworm. *Heredity (Edinb)*. **116**, 75–83  
370 (2016).
- 371 16. Beldade, P., Saenko, S. V, Pul, N. & Long, A. D. A gene-based linkage map for *Bicyclus*  
372 *anyana* butterflies allows for a comprehensive analysis of synteny with the lepidopteran  
373 reference genome. *PLoS Genet.* **5**, e1000366 (2009).
- 374 17. Šíchová, J. *et al.* Fissions, fusions, and translocations shaped the karyotype and multiple sex  
375 chromosome constitution of the northeast-Asian wood white butterfly, *Leptidea amurensis*.  
376 *Biol. J. Linn. Soc.* **118**, 457–471 (2016).
- 377 18. Al-Shahrour, F. *et al.* Selection upon genome architecture: Conservation of functional  
378 neighborhoods with changing genes. *PLoS Comput. Biol.* **6**, (2010).
- 379 19. Gordon, J. L., Byrne, K. P. & Wolfe, K. H. Mechanisms of chromosome number evolution in  
380 yeast. *PLoS Genet.* **7**, 0–3 (2011).
- 381 20. Coghlan, A., Eichler, E. E., Oliver, S. G., Paterson, A. H. & Stein, L. Chromosome evolution  
382 in eukaryotes: A multi-kingdom perspective. *Trends Genet.* **21**, 673–682 (2005).
- 383 21. Levis, R. W., Ganesan, R., Houtchens, K., Tolar, L. A. & Sheen, F. miin. Transposons in  
384 place of telomeric repeats at a *Drosophila* telomere. *Cell* **75**, 1083–1093 (1993).
- 385 22. Muller, H. J. The remaking of chromosomes. *Collect. net* **13**, 181–198 (1938).
- 386 23. Maddox, P. S., Oegema, K., Desai, A. & Cheeseman, I. M. ‘Holo’er than thou: Chromosome  
387 segregation and kinetochore function in *C. elegans*. *Chromosom. Res.* **12**, 641–653 (2004).
- 388 24. Lorkovic, Z. The genetics and reproductive isolating mechanisms of the *Pieris napi* -  
389 *bryoniae* group. *J. Lepid. Soc.* **16**, 5–19 (1955).
- 390 25. Maeki, K. & Kawazoe, A. On the Hybridization between Two Karyotype Lineages of *Pieris*  
391 *napi* Linnaeus from Japan. *Cytologia (Tokyo)*. **59**, (1994).
- 392 26. Buchfink, B., Xie, C. & Huson, D. H. Fast and sensitive protein alignment using  
393 DIAMOND. *Nat. Methods* **12**, 59–60 (2014).
- 394 27. Nallu, S. *et al.* The Molecular Genetic Basis of Herbivory between Butterflies and their Host-  
395 Plants. *bioRxiv* (2017). doi:10.1101/154799
- 396 28. Clark, A. G. *et al.* Evolution of genes and genomes on the *Drosophila* phylogeny. *Nature* **450**,  
397 203–218 (2007).
- 398 29. Aljanabi, S. M. & Martinez, I. Universal and rapid salt-extraction of high quality genomic  
399 DNA for PCR-based techniques. *Nucleic Acids Res.* **25**, 4692–4693 (1997).



- 400 30. Bentley, D. R. *et al.* Accurate whole human genome sequencing using reversible terminator  
401 chemistry. *Nature* **456**, 53–59 (2008).
- 402 31. Putnam, N. H. *et al.* Chromosome-scale shotgun assembly using an in vitro method for long-  
403 range linkage. *Genome Res.* **26**, 342–350 (2016).
- 404 32. Leggett, R. M., Clavijo, B. J., Clissold, L., Clark, M. D. & Caccamo, M. NextClip: an  
405 analysis and read preparation tool for Nextera Long Mate Pair libraries. *Bioinformatics* **30**,  
406 566–8 (2014).
- 407 33. Gnerre, S. *et al.* High-quality draft assemblies of mammalian genomes from massively  
408 parallel sequence data. *Proc. Natl. Acad. Sci.* **108**, 1513–1518 (2011).
- 409 34. Parra, G., Bradnam, K. & Korf, I. CEGMA: a pipeline to accurately annotate core genes in  
410 eukaryotic genomes. *Bioinformatics* **23**, 1061–1067 (2007).
- 411 35. Boetzer, M., Henkel, C. V., Jansen, H. J., Butler, D. & Pirovano, W. Scaffolding pre-  
412 assembled contigs using SSPACE. *Bioinformatics* **27**, 578–579 (2011).
- 413 36. Rastas, P., Calboli, F. C. F., Guo, B., Shikano, T. & Merilä, J. Construction of Ultradense  
414 Linkage Maps with Lep-MAP2: Stickleback F2 Recombinant Crosses as an Example.  
415 *Genome Biol. Evol.* **8**, 78–93 (2015).
- 416 37. Li, H. Aligning sequence reads, clone sequences and assembly contigs with BWA-MEM. **0**,  
417 1–3 (2013).
- 418 38. Li, H. *et al.* The Sequence Alignment/Map format and SAMtools. *Bioinformatics* **25**, 2078–  
419 2079 (2009).
- 420 39. Kvist, J. *et al.* Flight-induced changes in gene expression in the Glanville fritillary butterfly.  
421 *Mol. Ecol.* **24**, 4886–4900 (2015).
- 422 40. Bushnell, B. BBTools. (2017). at <<https://jgi.doe.gov/data-and-tools/bbtools/>>
- 423 41. Pages H, Gentleman R, Aboyoun P, et al. Biostrings: String objects representing biological  
424 sequences, and matching algorithms. *R Packag. version 2*, 2008 (2008).
- 425 42. Zdobnov, E. M. *et al.* OrthoDB v9.1: Cataloging evolutionary and functional annotations for  
426 animal, fungal, plant, archaeal, bacterial and viral orthologs. *Nucleic Acids Res.* **45**, D744–  
427 D749 (2017).
- 428 43. Shimomura, M. *et al.* KAIKObase: an integrated silkworm genome database and data mining  
429 tool. *BMC Genomics* **10**, 486 (2009).
- 430 44. Altschul, S. F. *et al.* Gapped BLAST and PSI-BLAST: a new generation of protein database  
431 search programs. *Nucleic Acids Res.* **25**, 3389–3402 (1997).
- 432 45. Kersey, P. J. *et al.* Ensembl Genomes 2016: More genomes, more complexity. *Nucleic Acids*  
433 *Res.* **44**, D574–D580 (2016).
- 434 46. Krzywinski, M. *et al.* Circos: An information aesthetic for comparative genomics. *Genome*  
435 *Res.* **19**, 1639–1645 (2009).

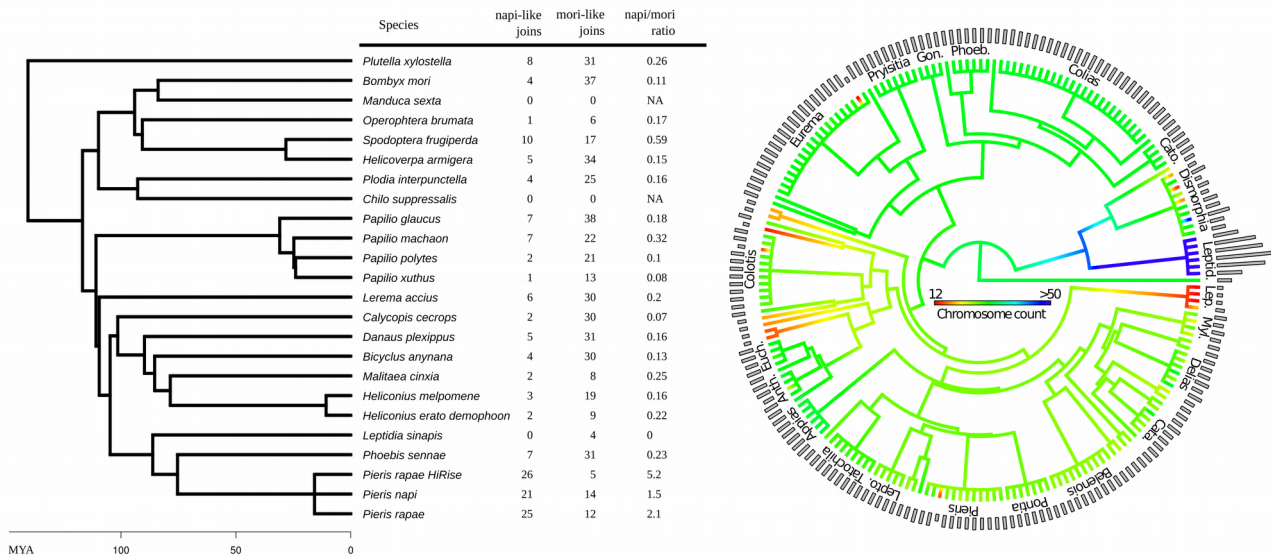


- 436 47. Challis, R. J., Kumar, S., Dasmahapatra, K. K., Jiggins, C. D. & Blaxter, M. Lepbase: The  
437 Lepidopteran genome database. *bioRxiv* 56994 (2016). doi:10.1101/056994
- 438 48. Wahlberg, N., Rota, J., Braby, M. F., Pierce, N. E. & Wheat, C. W. Revised systematics and  
439 higher classification of pierid butterflies (Lepidoptera: Pieridae) based on molecular data.  
440 *Zool. Scr.* **43**, 641–650 (2014).
- 441 49. Edger, P. P. *et al.* The butterfly plant arms-race escalated by gene and genome duplications.  
442 *Proc. Natl. Acad. Sci.* **112**, 8362–8366 (2015).
- 443 50. Lukhtanov, V. A. Karyotype evolution and systematics of higher taxa of Pieridae  
444 (Lepidoptera) of the World. *Ent. Obozr.* **70** 619–636, 3 figs (1991).
- 445 51. Revell, L. J. phytools: An R package for phylogenetic comparative biology (and other  
446 things). *Methods Ecol. Evol.* **3**, 217–223 (2012).
- 447 52. Narasimhan, V. *et al.* BCFtools/RoH: A hidden Markov model approach for detecting  
448 autozygosity from next-generation sequencing data. *Bioinformatics* **32**, 1749–1751 (2016).
- 449 53. Danecek, P. *et al.* The variant call format and VCFtools. *Bioinformatics* **27**, 2156–2158  
450 (2011).
- 451 54. Purcell, S. *et al.* PLINK: A Tool Set for Whole-Genome Association and Population-Based  
452 Linkage Analyses. *Am. J. Hum. Genet.* **81**, 559–575 (2007).
- 453 55. The UniProt Consortium. UniProt: a hub for protein information. *Nucleic Acids Res.* **43**,  
454 D204–12 (2015).
- 455 56. Alexa A and Rahnenfuhrer J. topGO: Enrichment Analysis for Gene Ontology. *R package*  
456 *version 2.26.0.* (2016). at <<http://bioconductor.org/packages/release/bioc/html/topGO.html>>
- 457 57. Dincă, V., Lukhtanov, V. A., Talavera, G. & Vila, R. Unexpected layers of cryptic diversity in  
458 wood white Leptidea butterflies. *Nat. Commun.* **2**, (2011).
- 459 58. Vila, R. *et al.* Phylogeny and palaeoecology of Polyommatus blue butterflies show Beringia  
460 was a climate-regulated gateway to the New World. *Proc. R. Soc. B Biol. Sci.* **278**, 2737–  
461 2744 (2011).
- 462 59. Lukhtanov, V. The blue butterfly Polyommatus (Plebicula) atlanticus (Lepidoptera,  
463 Lycaenidae) holds the record of the highest number of chromosomes in the non-polyploid  
464 eukaryotic organisms. *Comp. Cytogenet.* **9**, 683–690 (2015).

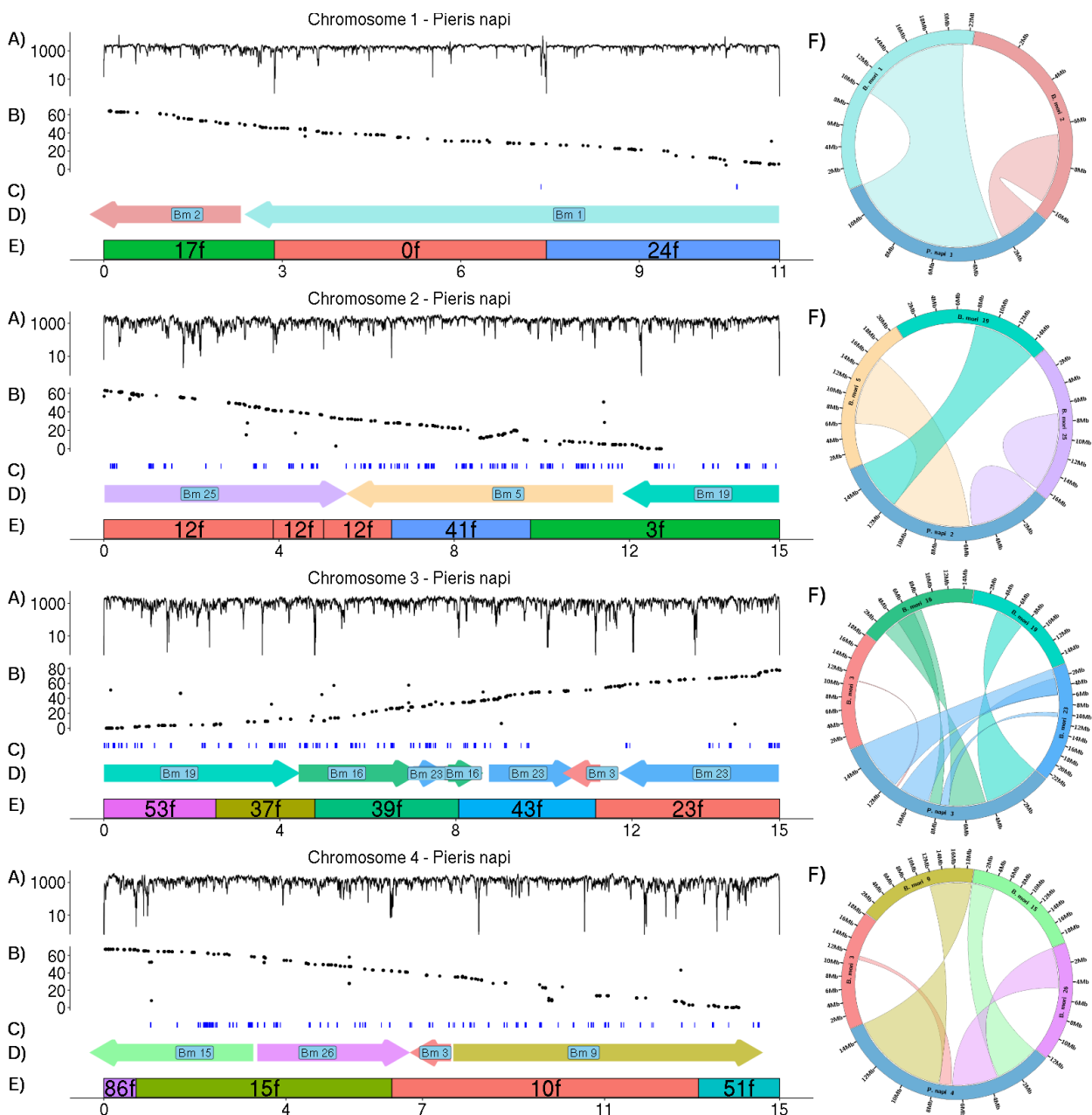


466 **Figure 1 a)** Chromosomal mapping between the moth *Bombyx mori* (Bombycoidea) and the  
 467 butterflies *Pieris napi* (Pieridae) and *Heliconius melpomene* (Nymphalidae). These species last  
 468 shared a common ancestor > 100 million generations ago<sup>49</sup>. Depicted are the reciprocal best hit  
 469 orthologs identified between *B. mori* and *P. napi* (n=2354) and between *B. mori* and *H. melpomene*  
 470 (n=2771). Chromosome 1 is the Z chromosome in *B. mori* and *P. napi* and 21 is the Z chromosome  
 471 in *H. melpomene*. Chromosomes 2-25 in *P. napi* are ordered in size from largest to smallest. Links  
 472 between orthologs originate from the *B. mori* chromosome and are colored by their chromosome of  
 473 origin, while *P. napi* chromosomes are colored blue and *H. melpomene* chromosomes are colored

474 orange. Links are clustered into blocks of synteny and each ribbon represents a contiguous block of  
 475 genes spanning a region in both species. **b)** Two largest autosomes of *P. napi* and their synteny to  
 476 other Lepidoptera and their phylogenetic relationship. The sister taxa and the more distant *B. mori*  
 477 share a high degree of macro synteny while the *P. napi* genome required multiple chromosomal  
 478 fusion and fission events to be patterned in the way that is observed. Band width for each species is  
 479 proportional to the length of the inferred chromosomal region of orthology, although the individual  
 480 chromosomes are not to scale.  
 481



482 **Figure 2 a)** A time calibrated phylogeny of currently available Lepidopteran genomes (n=24) and  
 483 estimates of their macrosynteny with *B. mori* and *P. napi*, with time in million years ago (MYA).  
 484 Macrosynteny was estimated by quantifying the number of times a scaffold of a given species  
 485 contained *B. mori* orthologs from two separate chromosomes and *P. napi* orthologs from a single  
 486 chromosome (napi-like join), or vice versa (mori-like joins)(see Supplemental Note for more  
 487 details). **b)** A time calibrated ancestral state reconstruction of the chromosomal fusion and fission  
 488 events across Pieridae (n=201 species). As only a time calibrated genus level phylogeny exists for  
 489 Pieridae, all genera with > 1 species are set to an arbitrary polytomy at 5 MYA, while deeper  
 490 branches reflect fossil calibrated nodes. The haploid chromosomal count of tips (histogram) and  
 491 interior branches (color coding) are indicated, with the outgroup set to n=31 reflecting the butterfly  
 492 chromosomal mode. Genus names are indicated for the larger clades (all tips labels in Supplemental  
 493 Material).



494

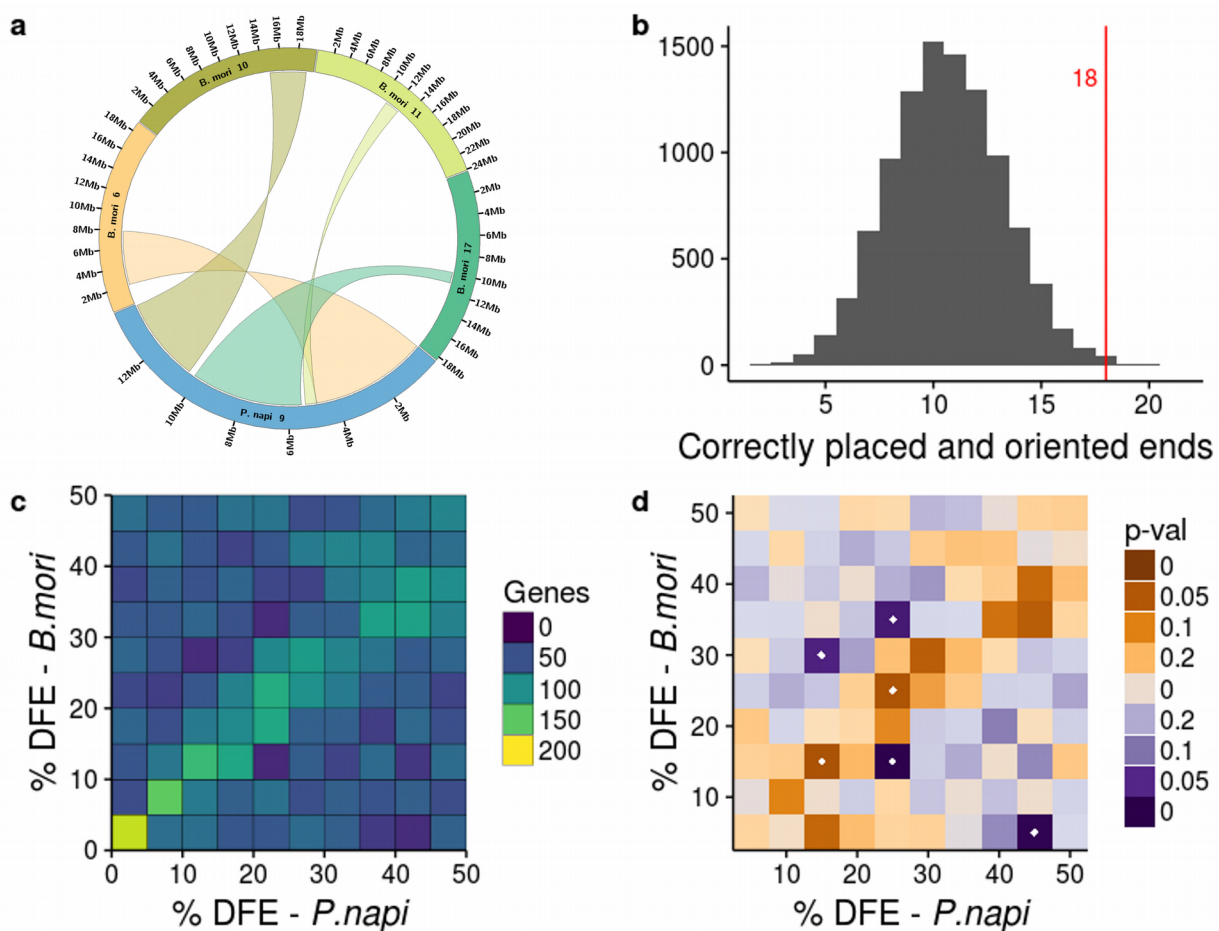
495

**Figure 3** Validation of syntenic relationship between *B. mori* and first four *P. napi* chromosomes. (a) Mate pair spanning depth across each chromosome summed for the 3kb, 7kb, and 40kb libraries. Spanning depths averaged 1356 across the whole genome. Of the scaffold join positions 74 of 97 were spanned by > 50 properly paired reads (mean = 117.8, S.D. = 298.7) which we considered good evidence for correct assembly at scaffold boundaries while the remaining 23 scaffold joins had 0 mate pair spans. (b) RAD-seq linkage markers and recombination distance along chromosomes from the first linkage map that was used for genome assembly. (c) Results from the second linkage map of maternally inherited markers, using RNA-Seq and whole genome sequencing. All markers within a chromosome are completely linked due to suppressed recombination in females (i.e. recombination distance is not shown on Y axis). (d) Syntenic block origin and orientation colored and labeled by the *B. mori* chromosome containing the orthologs, as in Fig. 1 (e) Component scaffolds of each chromosome labeled to indicate scaffold number and orientation. (f) To the right of each *P. napi* chromosome is a circos plot showing the location and orientation of syntenic blocks within each *B. mori* chromosome that comprise a given *P. napi* chromosome. Ribbons representing the blocks of synteny are colored by their orthologs location in the *B. mori* genome. Relative orientation of a block is shown by whether the ribbon contains a twist. Remaining chromosomes shown in Supplementary Fig. 2.

511

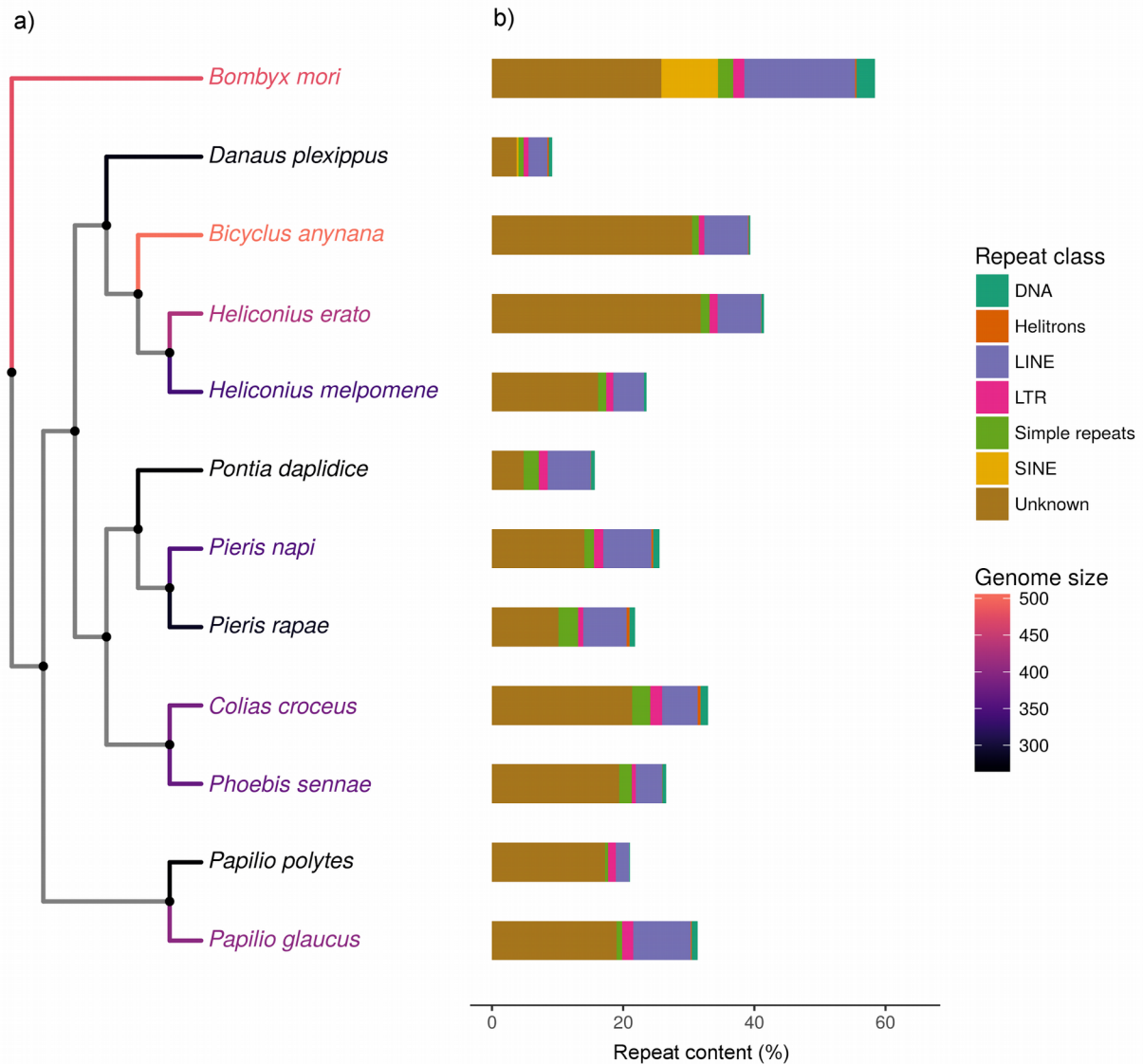
512  
513  
514  
515  
516





517  
518

519 **Figure 4.** Comparison of gene content of and chromosomal location of syntenic blocks between  
 520 *Pieris napi* and *Bombyx mori* in observed and randomly generated expectation genomes. (a)  
 521 Observed pattern of conserved syntenic block location within *P. napi* Chromosome 9, wherein  
 522 telomere facing and interior syntenic blocks are conserved between species despite shuffling. (b)  
 523 Histogram of the number of syntenic blocks that are terminal on the *B. mori* genome and also occur  
 524 in the terminal position on chromosomes in a simulated genome, from 10,000 simulated genomes  
 525 (average 10.7, std dev= 6.8). (c) Percentage distance from the end (DFE) of a chromosome of a  
 526 single copy gene in *P. napi* vs. DFE of that gene's single copy ortholog (SCO) in *B. mori*. Counts  
 527 binned on the color axis. (d) Comparison between the observed DFE distribution and the expected  
 528 distribution generated from 10,000 genomes of 25 chromosomes constructed from the random  
 529 fusion of syntenic blocks. Bins in which more genes occur in the observed genomes than the  
 530 expected distribution are in orange, less genes in blue,  $P < 0.05$  in either direction are denoted by a  
 531 white dot. SCO spatial distribution was significantly higher than expected along the diagonal (two  
 532 bins with  $p < 0.05$ ), while significantly lower than expected off the diagonal (four bins with  $p <$   
 533 0.05).



534  
535 **Figure 5.** The genomic size and repeat content of Lepidopteran genomes placed in a phylogenetic  
536 context. (a) Phylogenetic relationships represented as a cladogram, with terminal branches and  
537 species names colored by genome size estimates from k-mer distributions of read data. (b) The  
538 fraction of repeat content of each genome, color coded by repeat class.